ELSEVIER

Journal of Photochemistry and Photobiology A: Chemistry 105 (1997) 55–63

Journal of
PHOTOCHEMISTRY
AND
PHOTOBIOLOGY
A:CHEMISTRY

Charge recombination reactions in self-assembled porphyrin-based ion-pair complexes

Stephan L. Logunov [1], Michael A.J. Rodgers *

Center for Photochemical Sciences, Department of Chemistry, Bowling Green State University, Bowling Green, OH 43403, USA

Received 23 April 1996; accepted 23 July 1996

Abstract

The dynamics of charge recombination (CR) reactions after photoinduced charge separation (CS) in self-assembled ion pairs of charged porphyrins and oppositely charged electron acceptors were studied in aqueous solution. In most cases the CS reaction occurs in times less than 0.1 ps after the photoexcitation event, whereas the CR reaction is slower, on the multipicosecond time scale. The CR reactions show an invariance of rate constant (ca. 10^{12} s^{-1}) with driving force at $\Delta G \leq 1.2$ eV. Moreover, the CR processes exhibited a strongly inverted dependence on driving force when $\Delta G > 1.3$ eV. The rate constants of CR reactions in the region independent of driving force were insensitive to changes in the longitudinal relaxation time of the solvent, as determined by changing the solvent from neat water to alcohol–water mixtures, which may indicate that the CR reaction rate in the driving force independent region is limited by vibrational relaxation in the ground state of the complex.

Keywords: Photoexcitation; Electron transfer; Solvent effects; Driving force dependence; Inverted region; Picosecond flash photolysis

1. Introduction

Water-soluble porphyrins with peripheral charged groups tend to form ion pairs with oppositely charged species in which electrostatic and dispersion forces are responsible for the self-assembly of this type of complex [1–3]. When the oppositely charged component molecules have planar π-systems, the molecules tend to stack in a face-to-face configuration [4], such that the π-orbitals of the macrocycles can interact sufficiently to cause fluorescence quenching [5–9]. Ion-pairing interactions of this nature can be useful for studying the rate constants of intra-complex charge separation (CS) and charge recombination (CR) reactions, and observing how these parameters depend on the structural and electronic properties of the complex. There are numerous studies of such types of complex [1–10]. The complexation reaction is simplicity itself, inasmuch as all that is required is to codissolve the two ionophoric species in water at the appropriate pH, temperature, and ionic strength. Subsequent illumination of the system leads to a rapid photoinduced electron transfer reaction (in the range of a few picoseconds) to form a radical pair state that then rapidly repopulates the ground state within the solvent cage. The mechanism is shown in Scheme 1.

In Scheme 1, D^{m+} represents a positively charged electron donor in the ground state, A^{n-} represents a negatively charged electron acceptor in its ground state, and the square brackets indicate that the species enclosed within is an electrostatically bound complex inside a solvent cage. With anionic porphyrins and cationic electron acceptors (i.e. viologens), the charges are reversed, but the ion-pairing concept is retained.

The rate constants of CS and CR reactions are expected to vary with changes in the driving force which can be controlled by structure-derived variations in the reduction potentials of D and A. To some extent the CS and CR rate constants may be influenced by the distribution of local electric fields induced by the peripheral charges on the complex components. Previously we have shown that in ion pairs of anionic

$$D^{m+} + A^{n-} \rightleftharpoons [D^{m+}{:}A^{n-}]$$

$$[D^{m+}{:}A^{n-}] \xrightarrow{h\nu} [D^{m+}{:}A^{n-}]^{*} \underset{k_{-1}}{\overset{k_{CS}}{\rightleftharpoons}} [D^{(m+1)+}{:}A^{(n+1)-}]$$

$$[D^{(m+1)+}{:}A^{(n+1)-}] \xrightarrow{k_{CR}} [D^{m+}{:}A^{n-}]$$

Scheme 1.

---

* Corresponding author.

[1] Current address: School of Chemistry and Biochemistry, Georgia Institute of Technology, Atlanta, GA 30332, USA.

1010-6030/97/$17.00
PII S1010-6030(96)04468-1

porphyrins with a variety of bipyridinium salts, a plot of the logarithm of the CR rate constant vs. driving force forms a homogeneous set of data with a marked inverted region when $\Delta G > 0.8$ V, and that there is a region which is independent of driving force at lower values of ΔG [10]. The data were treated in terms of adiabatic electron transfer controlled by solvent dynamics [10]. In the present study we have extended the range of driving force, employed a different set of donor–acceptor couples, studied the effect of changing the solvent, and improved our time resolution in order to investigate the dynamics of CS reactions. These new data force us to draw different conclusions about what factors control the electronic motions. The geometry of the complex is discussed, based on comparison of the data sets for the rate of the CR reaction vs. driving force for solvent-separated (SS) and contact ion pairs (CIP).

2. Materials and methods

2.1. Materials

Meso-tetrakis(4-sulfonatophenyl)porphyrin tetra-sodium salt (H_2TPPS) and uroporphyrin dihydrochloride (H_2Up) were used as received from Porphyrin Products. Meso-tetrakis(*N*-methyl-4-pyridinium)porphyrin tetrachloride (H_2TMPyP) and the Mg and Zn metallo-derivatives of H_2TPPS and H_2TMPyP were used as received from Midcentury Chemicals. Metallo-derivatives of H_2Up were prepared as described previously [10–12]. Methylviologen (MV^{2+}), benzylviologen (BV^{2+}) and 2,2′-azinobis(3-ethylbenzothiazoline) sulfonic acid (AZ) were used as received from Sigma. Other bipyridinium salts such as triquat, tetraquat, dimethyltetraquat and phenathrolino[4,5-a:6,7-c]diazepinediium salt were prepared in accordance with literature procedures [12,13]. The disodium salts of 9,10-anthaquinone-2,6 disulfonate and 9,10-anthraquinone-1,5 disulfonate were used as received from Fluka. The water and organic solvents used to prepare solutions were reagent grade. Where indicated, the ionic strength was adjusted by the addition of sodium chloride.

2.2. Time-resolved measurements

The picosecond absorption spectrometer employing an Nd:YAG laser (Quantel 571C) with 30 ps pulse duration and excitation wavelength of 532 nm has been described [14]. Briefly stated, the transient difference spectra were obtained using the pump-probe method in which the pump was the 532 nm pulse and the probe was a coherent continuum generated by focusing the residual 1064 nm light into a 10 cm cuvette containing a 1:1 D_2O:H_2O mixture. The white beam was split into two beams to generate a double-beam system. After passing through the excited volume, one probe beam was dispersed in a grating spectrograph, at the focal plane of which was a linear array detector with two arrays in the same package. The second probe beam passed through an unirradiated region of the sample and was again dispersed and displayed on the other array in the detector. Absorption spectra were generated by calculating the ratios of the diode array amplitudes diode-by-diode after appropriate calibration and balancing. Time-delayed spectra and kinetic information were obtained by optically delaying the arrival of the pump beam at the sample with respect to the probe beam.

For measurements of charge separation and recombination processes where even higher time resolution was required, a femtosecond flash photolysis unit was employed [6,15]. In this case the source of the 250 fs pulses was a two-jet ring dye laser oscillator augmented with four stages of amplification. A double grating system was employed for compression of the 630 nm amplified pulse. In some cases it was necessary to use an excitation wavelength of 580 nm, in which case the duration of the pulse was ca. 400 fs [16]. In all measurements the energy of the excitation laser pulse was sufficient to excite about 20%–30% of the molecules present in the ground state.

Time-resolved fluorescence measurements were performed using a time-correlated single-photon-counting system with an instrument response function of ca. 500 ps [17]. The excitation wavelength was obtained by tuning a synchronously pumped, mode-locked, cavity-dumped dye laser to 580 nm.

2.3. Steady-state measurements

Fluorescence spectra were recorded with a Perkin-Elmer LS5B spectrofluorimeter and ground state absorption spectra were obtained using a Perkin-Elmer 3840 diode array UV–visible spectrophotometer. All experiments were carried out at room temperature (21 ± 1 °C).

3. Results and discussion

In aqueous solutions at low ionic strength (les than 1 mM), highly charged porphyrin species such as the TPPS and TMPyP families tend to associate strongly in ion-pairing interactions with oppositely charged substrates. In this way it becomes possible to arrange for self-assembly of putative electron donor–acceptor pairs that are closely coupled in the ground states prior to photoexcitation. It is the photoexcitation event that provides the initial state with the driving force necessary to achieve charge separation. This principle of self-assembly through ion-pairing interactions is identical with the earlier work from this laboratory in which electron transfer reactions were initiated within self-assembled units composed of derivatives of cytochrome-*c* and various uroporphyrins [11]. In that work the molecular geometry — largely determined by the protein — ensured that electron transfer (forward and reverse) occurred over a distance of some 8 Å. Here the donor and acceptor pairs are situated much closer to each other. In the following we present evi-

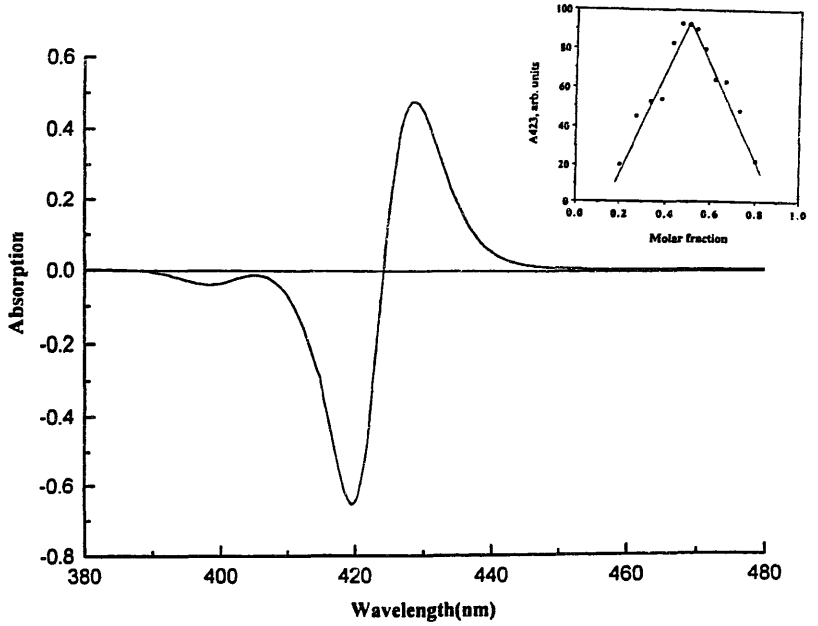

Fig. 1. Difference absorption spectrum of 1 M H_2TPPS obtained after adding 1 mM MV^{2+}. Measurements were taken in aqueous solution using a 1 cm tandem cell. The inset is a Job plot, obtained at 423 nm, for H_2TPPS and MV^{2+}. The total concentration was 5 μM.

dence for the formation of ion-pair complexes in the ground state, following which we outline their behavior on photoexcitation.

3.1. Fluorimetric and steady-state absorption experiments

Fig. 1 shows a differential optical absorption spectrum in the Soret band region of H_2TPPS with the addition of MV^{2+}. The strong positive peak at 425 nm indicates a significant interaction between the ground state components and is consistent with complex formation. The inset to Fig. 1 is a Job plot of absorbance at 425 nm vs. the fractional composition of the solution components at constant total concentration. This indicates a 1:1 stoichiometry for the complex between H_2TPPS and MV^{2+}. Measurements of the fluorescence intensity of aqueous solutions containing ZnTPPS (1 μM) and bipyridinium salts resulted in linear Stern–Volmer plots as exemplified in Fig. 2(A). The evaluated Stern–Volmer constant K_{SV} was 2.2×10^4 M^{-1}, which is close to the value of 1.5×10^4 M^{-1} reported [2] for the same system. Taking the lifetime of the porphyrin singlet state as 1.7 ns [3] leads to a bimolecular reaction rate constant for the quenching of the porphyrin fluorescence of 1.4×10^{13} M^{-1} s^{-1}. This is highly improbable for a dynamic quenching event, and the clear indication is that bimolecular events are not operating in this concentration range and that the observed quenching corresponds to a static process that arises from the coproximity of the porphyrin and the viologen prior to light absorption. These data are consistent with earlier results which indicated that, depending on the extent of complexing, both static and dynamic quenching can occur in aqueous media containing complexes of this type [1–10]. Time-resolved fluorescence lifetime measurements (not shown here) indicate that only about 20%–30% of fluorescence quenching at millimole quencher concentration is due to the bimolecular dynamic process with a rate constant of 1×10^{11} M^{-1} s^{-1}. The remainder is due to static quenching which deactivates the excited state in times much less than the system time resolution (see below).

When using cationic porphyrins, a few complications may arise. There are a lot of contradictions in the literature regarding the aggregation of TMPyP porphyrins in water [18–20]. Very recently Vergeldt et al. [19] suggested that at concentrations less than 10^{-3} M, all porphyrins are in monomeric

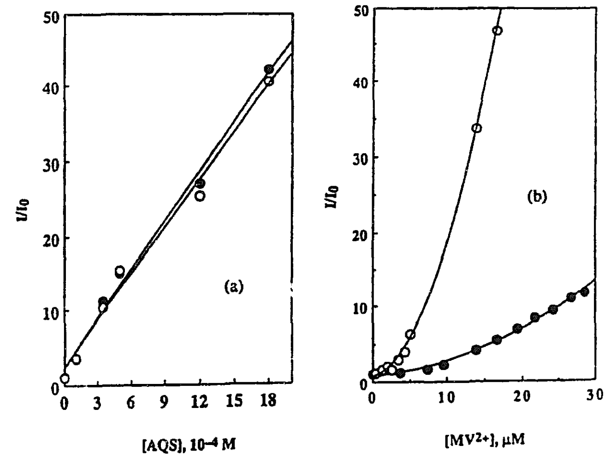

Fig. 2. (A) Stern–Volmer plot for the fluorescence quenching of ZnTPPS (1 μM) by MV^{2+} in water. Measurements were taken at two wavelengths, corresponding to the maxima of the fluorescence spectrum; ○ 650 nm, ● 610 nm. The solid lines are best fits with $K_{SV}=2.2\times10^4$ M^{-1} for 610 nm and 2.1×10^4 M^{-1} for 650 nm. ZnTPPS was excited at 560 nm. (B) Stern–Volmer plot for the fluorescence quenching of $H_2TMPyP(Cl)$ (1 μM) by AQS(2,6) in water (○) and in a 50% v/v mixture of water with ethanol (●). The solid lines are best fits to Eq. (1).

form, and all effects which were previously thought to be due to the aggregations are, in fact, absorption of the porphyrin by the quartz material of the cuvette. Stern–Volmer plots of the fluorescence intensity from aqueous solutions of MTMPyP and AQS(2,6) show non-linear behavior (Fig. 2(B)). This is similar to results reported earlier [20]. Assuming that all complexes between MTMPyP and AQS are non-fluorescent, and that a combination of 1:1 and 1:2 complexes exists, and that fluorescence arises only from the fraction of uncomplexed porphyrin present at equilibrium, then it is possible to describe the fluorescence intensity behavior by

$$I/I_0 = 1 + K_1[\mathrm{AQS}] + K_1K_2[\mathrm{AQS}]^2 \quad (1)$$

where K_1 and K_2 are equilibrium constants for the processes

$$\mathrm{TMPyP} + \mathrm{AQS} \rightleftharpoons \mathrm{TMPyP \cdot AQS}$$

$$\mathrm{TMPyP \cdot AQS} + \mathrm{AQS} \rightleftharpoons \mathrm{TMPyP \cdot 2AQS}$$

and [AQS] is the concentration of uncomplexed AQS. Eq. (1) will be valid for AQS concentrations significantly in excess of the porphyrin concentration. The curved lines in Fig. 2(B) are fits of Eq. (1) to the data. The parameters $K_1 = 1.8 \times 10^5\ \mathrm{M}^{-1}$ and $K_2 = 9 \times 10^5\ \mathrm{M}^{-1}$ resulted from these fits (Table 1). Thus, under our experimental conditions, the system contains largely 1:2 complexes. In the case of the AQS(1,5) isomer, the Stern–Volmer plots were linear with $K_{SV} = 1.1 \times 10^4\ \mathrm{M}^{-1}$. This behavior suggests that the structure of the complex is 1:1, i.e. a single AQS molecule associated with a porphyrin dimer.

3.2. Bimolecular reactions between porphyrin triplet states and selected quenchers

Fig. 3 depicts a kinetic profile of the transient behavior of an aqueous solution of ZnTPPS (1 μM) containing 10 μM MV^{2+}. Under these conditions, about 20% of the porphyrin will be in a ground state complex with MV; the rest will be free porphyrin. Excitation was at 532 nm with an 8 ns laser pulse. The displayed profile was recorded at 420 nm in the Soret band of the porphyrin, and it shows an instantaneous bleaching of the porphyrin ground state, followed by an exponential recovery to a non-zero baseline. Similar kinetic profiles were observed with ZnTPPS and a series of bipyridinium acceptors, and for H_2TMPyP and AQS ions as reacting pairs. At this wavelength (420 nm) the extinction coefficient of the porphyrin ground state is much greater than that of the triplet state [21], which is formed within a few nanoseconds of excitation [2]. Subsequently, the excited triplet state will be quenched by bipyridinium ions present in the solution, with the concomitant formation of the radical pair. This reaction is diffusion controlled [22,23] and is kinetically first order. The kinetic scheme that outlines the charge separation and recombination processes for the separated and uncomplexed reactant states can be understood according to Scheme 2.

Table 1

Association constants for self-assembled ion pair complexes

Porphyrin	Quencher	K_1 (M^{-1})	K_2 (M^{-1})
ZnTPPS	MV	2.2×10^4	–
H_2TMPyP	AQS(2,6)	1.8×10^5	9.0×10^5
H_2TMPyP	AQS(2,6) [a]	9.7×10^4	1.2×10^5
ZnTMPyP	AQS(2,6)	1.88×10^6	1.0×10^7
ZnTMPyP	AQS(2,6) [a]	1.2×10^5	1.1×10^5
H_2TMPyP	AQS(1,5)	1.1×10^4	–
H_2TMPyP	AZ	4.7×10^4	–

[a] Measurements were taken in a 50% mixture by volume of water and ethanol.

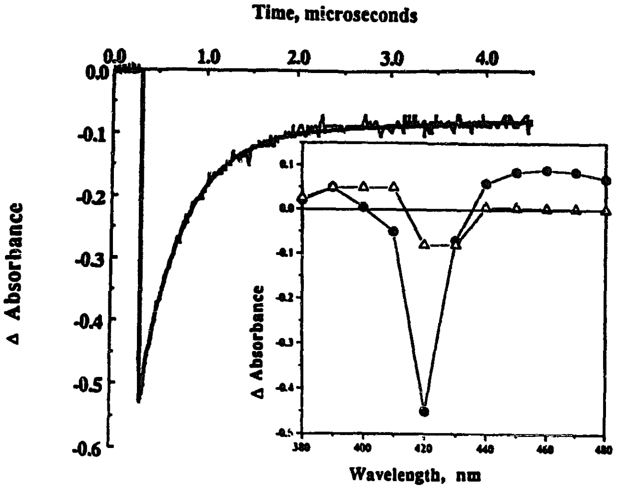

Fig. 3. Time profile of the absorbance changes at 420 nm after excitation of an aqueous solution of ZnTPPS (1 μM) by an 8 ns laser pulse at 532 nm in the presence of 10^{-4} M MV^{2+}. The inset shows difference absorption spectra measured for the above solution at 100 ns (●) and 4 μs (Δ) after excitation.

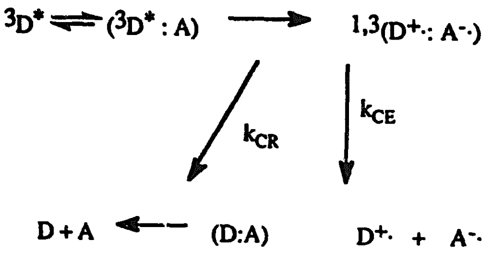

Scheme 2.

Formed in this manner, the radical pair is solvent separated and can escape from the solvent cage to form a pair of uncorrelated radicals in competition with CR inside the cage [22,23]. These uncorrelated radicals will diffuse throughout the bulk medium, encountering each other in normal random diffusive events, and mutually annihilate, eventually restoring the initial reactant condition. The recovery of the ground state due to this extra-cage radical recombination reaction will be kinetically second order. Thus, the total kinetic behav-

---

[2] Under the prevailing low ionic strength (less than 10^{-3} M), some porphyrin-quencher ion-pairing occurs. However, as Fig. 2(A) shows, at the quencher concentrations employed (0.01 mM), this corresponds to only about 20% of the total porphyrin being complexed. The observed T1 state kinetics arise from the majority of porphyrin states in non-complexed form.

ior at the Soret band will be a combination of first- and second-order processes, the former following the in-cage ground state recovery process k_{CR}, and the latter the extra-cage process. The trace in Fig. 3 depicts this behavior. Using data of the type depicted in Fig. 3, it is possible to extract the fraction of ion pairs that escape the solvent cage F_{CE} as being equal to the ratio of the amplitude of the second-order component, extrapolated to $t=0$, to the total initial amplitude of the bleaching signal. Then it follows that

$$F_{CE}=k_{CE}/(k_{CE}+k_{CR})$$

or

$$k_{CR}=k_{CE}(1-F_{CE})/F_{CE}$$

where the rate constants are as indicated in Scheme 2. A similar analysis was used by Mataga and coworkers [22,23]. The experiments were carried out with ZnTPPS as putative donor, coupled with a series of bipyridinium salts having the same +2 total charge. In such a case, it seems safe to assume that k_{CE} will be independent of the nature of the acceptor. From the measurements of F_{CE} for the several bipyridinium acceptors, the ratio k_{CR}/k_{CE} was evaluated for each couple. A plot of $\log(k_{CR}/k_{CE})$ vs. driving force for the bimolecular process is presented in Fig. 4.

With k_{CE} invariant, the dependence of the charge recombination rate constant k_{CR} against driving force for the reaction was determined and plotted. This is shown in Fig. 4, where it can be seen that the reorganization energy for this reaction in water solution is about 1.3 eV, which includes values of the internal reorganization energies of 0.1 eV for the porphyrin [24,25] and 0.1 for the viologens. A similar experimental series for TMPyP and anthraquinones resulted in a plot that was shifted to higher reorganization energies (Fig. 4). This probably arises from an increased internal reorganization energy for anthraquinone of 0.2 eV [26,27]. There should be no difference in solvent reorganization energy for this type of solvent-separated pair, even when the charges on donor and acceptor are reversed. We therefore conclude from these experiments that the solvent reorganization energy involved in the collapse of solvent-separated ion pairs of the type studied here in aqueous solution is 1.0±0.1 eV. This corresponds to values of 0.6–1.0 eV for porphyrin-like species [25].

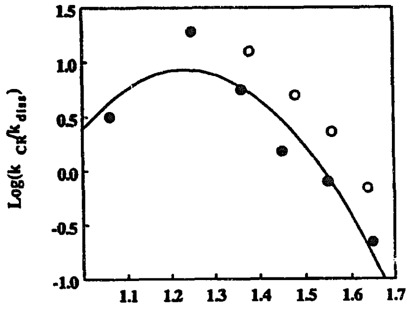

Fig. 4. Plot of $\log(k_{CR}/k_{CE})$ vs. driving force for the bimolecular CR reactions. Open circles correspond to quenching of the ZnTPPS triplet state by a series of bipyridinium salts and AZ; closed circles correspond to quenching of the ZnTMPyP triplet state by AQS. The parabolic fit for the series of CR reactions for the ZnTPPS complexes was obtained using the relationship $\log k_{CR}=\exp(-(\Delta G-\lambda)^2/4k_BT)+C$, where ΔG is the driving force for the reaction (the difference between the reduction potentials of the acceptor and donor), λ is the reorganization energy, k_B is the Boltzmann constant, C is a constant.

3.3. Photoexcitation of ion-pair complexes

In the absence of acceptors, ultrafast laser photolysis of aqueous porphyrin solutions resulted in the instantaneous formation of intense $S_1 \rightarrow S_n$ absorbance bands in the 400–800 nm region. The spectra showed the characteristic minima at the wavelengths of ground state absorbance corresponding to loss of the porphyrin ground states. In addition, at the wavelengths where the $S_1 \rightarrow S_0$ radiative transition occurs, a minimum arising from the superposition of stimulated emission was noted [28]. When acceptor species were present under conditions of complexation with porphyrins such that the majority of the porphyrin species were complexed, the stimulated emission was absent and the absorbance from $S_1 \rightarrow S_n$ transitions was replaced at earliest times by a new absorption that could be identified as being due to the ion-radical pair [21,29] (Fig. 5). We showed previously that for a series of anionic MTPPS porphyrins and bipyridinium compounds [10] the lifetime of the CR reaction varied from 1 to 450 ps and exhibited a dependence on the reduction potentials of the donor and acceptor. Even with a 400 fs laser pulse, we could not resolve the CS reaction, indicating that it has to be shorter than 100–200 fs, if it is not instantaneous.

In the case of cationic porphyrins, similar behavior could be observed. On photoexcitation of an aqueous solution of H_2TMPyP ($A_{532}=0.5$ per cm), a difference spectrum corresponding to the $S_1 \rightarrow S_n$ absorption is observed. Absorption bands at 530, 560, 580, and 640 nm (Fig. 5(A)) arise from bleaching of the ground state, and the band at 720 nm, in the

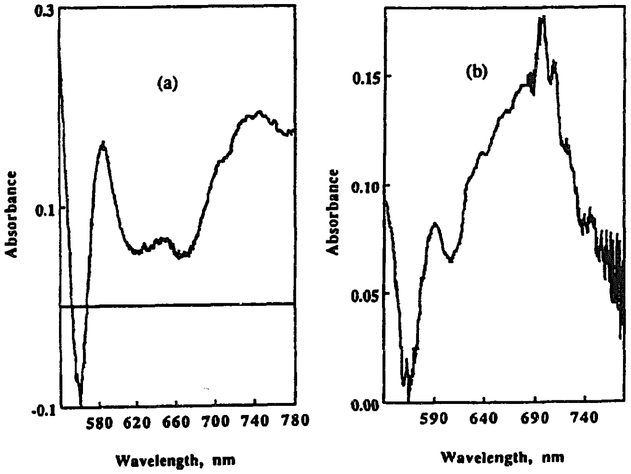

Fig. 5. (A) Difference absorption spectrum obtained immediately after excitation of a 10 μM aqueous solution of H_2TMPyP by a subpicosecond 600 nm laser pulse. (B) Difference absorption spectrum obtained immediately after excitation of a 10 μM aqueous solution of H_2TMPyP in the presence of 100 μM AQS(2,6) by a 30 ps laser pulse at 532 nm.

same sense as an absorption signal, is due to stimulated emission from S_1. The addition of 2×10^{-5} M AQS(2,6) as electron acceptor causes absorbance spectral changes that are attributed to radical–ion pair spectra [7,21,29] (Fig. 5(B)). The positive band at 700 nm is characteristic of the cation radical of the TMPyP [7,29]. The same effect was obtained when complexes of AQS(1,5) with MgTMPyP or ZnTMPyP were excited. The decay of the radical pair was found to be monoexponential. Kinetic data for the CR reactions are collected in Table 2.

In order to isolate the efect of solvent on the rates of CS and CR reactions, it is necessary to use a complex having a driving force for electron transfer that lies in the region where the rate constant is virtually independent of the driving force of the reaction. This occurs where the plot of log k vs. ΔG exhibits zero slope. For this experiment the complex of TMPyP as electron acceptor ($E_A{}^*/_{A^-}=0.23$ eV) with 2,2′-azinobis(3-ethylbenzothiazoline) sulfonic acid (AZ) as electron donor ($E_{D^+/D}=-0.45$ eV) was chosen [33], yielding a driving force of 0.68 for the CR reaction of the complex (without correction for electrostatic interaction between donor and acceptor). This value is in the required region (see later). The Stern–Volmer behavior for the quenching of the porphyrin fluorescence is very similar to that of TPPS-type porphyrins complexed with bipyridinium salts, where the quenching is mostly static.

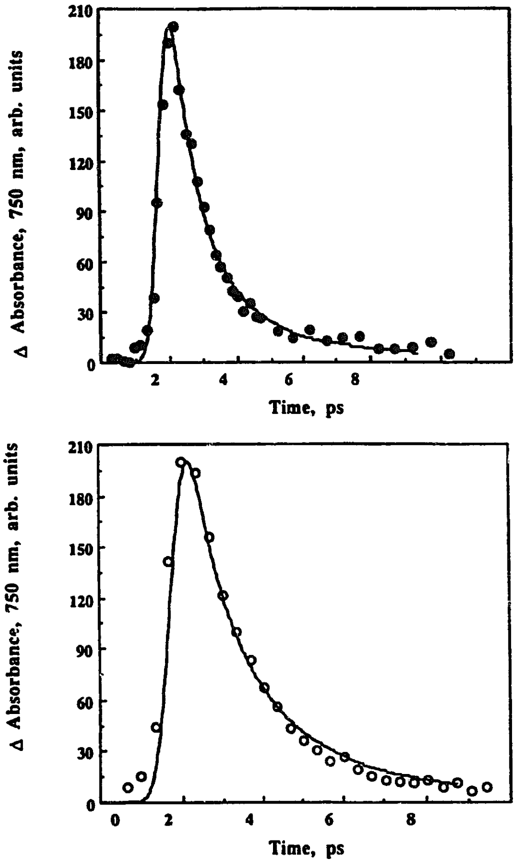

Fig. 6. A kinetic profile at 750 nm resulting from excitation at 600 nm of the complex between H_2TMPyP and AZ in aqueous solution (●) and in a 1:1 by volume mixture of water and 1-propanol (○).

Table 2
Rate constants and driving force for charge recombination reactions in complexes containing TMPyP

Electron donor	Electron acceptor	Rate constant (10^{11} s^{-1})	Driving force [a] (eV)
H_2TMPyP	AQS(2,6)	0.83	1.78
ZnTMPyP	AQS(2,6)	3.3	1.56
ZnTMPyP	AQS(1,5)	0.5	1.7
H_2TMPyP	AQS(1,5)	0.15	1.82
MgTMPyP	AQS(2,6)	9.0	1.46
MgTMPyP	AQS(1,5)	2.0	1.6
PdTMPyP	AQS(2,6)	1.0	1.8
AZ	H_2TMPyP	3.0 [b]	0.68
AZ	ZnTMPyP	2.0 [b]	1.3

[a] Data for the driving force were calculated as the sum of oxidation and reduction potentials of donor and acceptor. Reduction potential values for porphyrins were taken from [29], those for AZ from [30,36], those for AQS from [26], and those for bipyridinium salts from [32].

[b] Average lifetime.

It was found that the formation of the CS state is instantaneous on photoexcitation, being complete within the laser pulse (400 fs). The kinetic profile of the CR reaction has two exponential components with lifetimes of 0.9 ± 0.25 ps and 3.0 ± 0.7 ps respectively (Fig. 6), while single exponential decays were observed for all complexes listed in Table 2. This effect is attributed to the different electronic interactions between donor and acceptor. In this case TMPyP is the electron acceptor and different molecular orbitals are involved in the CS and CR processes. The electronic coupling between the states may be different from those cases where the porphyrin S_1 state is the donor. A similar effect was reported for the benzene–Br ion pair [34] when distribution of the CR rate constant was found to vary from 10^{12} to 10^9 s^{-1}. In our case the distribution of the CR rate constants is very narrow, suggesting that the variations in the geometry of the complex are not significant. The average lifetime of the CR reaction was calculated to be 1.1 ps; that is close to the maximum of the rate constants measured for other complexes studied. Thus, it was concluded that there is no significant difference in the electronic coupling when the TMPyP entity is either donor or acceptor. The small changes in the driving force for charge recombination induced by solvent changes around the TMPyP-AZ complex do not cause any significant differences in the rate of CR since the reaction is virtually independent of ΔG at these driving force values. Therefore, any observed changes in rate constant will arise from changes in the solvent relaxation time, assuming the same geometry of the complex. The relaxation dynamics of pure water and 1-propanol are very different, and the longitudinal relaxation times for these solvents are 0.2 ps and 100 ps respectively [35]. Flash photolysis of the TMPyP–AZ complex in a mixture of 1-propanol and water (50% v/v) indicated that the dynamics of the CR reaction were biexponential with lifetimes equal to 1.0 ± 0.2 ps and 3.2 ± 0.2 ps. The average lifetime equals 1.6 ps, only

1.5 times longer than the value in neat water. If the 1-propanol–water mixture were ideal, the longitudinal relaxation time for the 50:50 mixture of the two solvents would be 6 ps, or 30 times longer than for neat water. It is very likely that the longitudinal relaxation time for the mixture is not a purely additive quantity, but the insensitivity of the lifetime of the CR process to the solvent dynamics suggests that electronic interaction between donor and acceptor and not solvent relaxation governs the kinetics [34]. These data points, together with the full set of data for the CR reactions within the complexes, are shown in Fig. 7 [3].

The composite plot of log k_{CR} vs. the driving force for CR ΔG in Fig. 7 shows a strong inverted region at driving forces in excess of approximately 1.2 eV, with a leveling out below this value. In this plot the driving force was calculated as the sum of oxidation and reduction potentials of the donors and acceptors of electrons. However, it requires some correction for the electrostatic interaction between the photogenerated electron and hole and the peripheral charges of both entities. Values of ΔG can be estimated from the relationship

$$\Delta G_{CR}=E_{A/A^-}+E_{D}{}^{*}/_{D^+}+\Delta CI \tag{3}$$

where ΔCI represents the changes in the Coulombic interaction (CI) that accompany charge recombination. Setting $\Delta CI=0$ in the above expression, all the data points for complexes between anionic porphyrins and cationic acceptors lie on a single curve (Fig. 7, open circles). Thus electron coupling between donor and acceptor in the case of TPPS and Up is invariant across the range. The tight structure of the complex and its ultrarapid rate of CR at the top of the curve suggest that the distance between donor and acceptor species is very small and corresponds to that in a contact ion pair (CIP) [23,30,36]. The rate constant values in the inverted region ($\Delta E > 1.3$ eV) are shifted to higher energies by 0.2 ± 0.01 eV for the cationic porphyrin–anionic acceptor (AQS) pairs. This effect is also mirrored in Fig. 4 for the bimolecular charge recombination reactions, where the shift is about 0.1 eV, and is probably the result of a difference in internal reorganization energy between the anionic and cationic acceptors caused by different distances between the ionic sites on viologens and sulfonated anthraquinones. However, the shift of the curve corresponding to the CIP (Fig. 7) is larger than the shift for the solvent-separated pairs (Fig. 4). This difference possibly arises, as mentioned above, from the Coulombic interaction, which is weaker in solvent-separated pairs than in CIP. As stated earlier, the stoichiometry of complexes containing MTMPyP and AQS(2,6) is probably not 1:1. In the case where two molecules of AQS(2,6) interact with a single porphyrin molecule, the interaction between the AQS(2,6) pair is expected to be much weaker than that between the porphyrin and AQS(2,6).

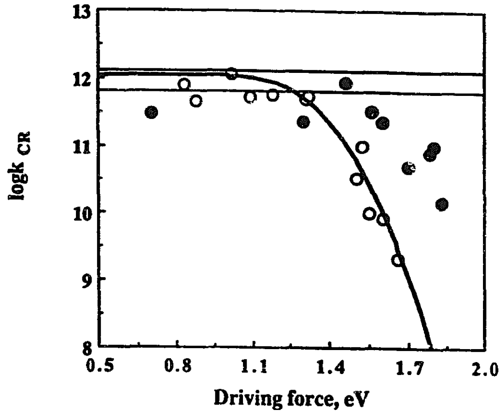

Fig. 7. A plot of log k_{CR} vs. driving force for complexes between anionic porphyrins and cationic electron acceptors (○, from [10]), and for complexes between TMPyP and anionic species (●, this work). The solid line corresponds to the fit of the open circle data to Eq. (4). The parameters are $V=0.15$ eV, $\lambda_v=0.2$ eV, $\lambda_s=0.45$ eV, $h\nu_v=1500$ cm^{-1}, $\tau_L=0.8$ ps. The horizontal lines are values of rate constants corresponding to lifetimes of 0.8 and 2 ps.

Having obtained the data presented in Fig. 7, it is interesting to employ them to test the current theories of electron transfer. Accordingly, an approach similar to that of Farid and coworkers [36] and of Jortner and Bixon [37] was employed which takes into consideration solvent relaxations having a Debye frequency spectrum:

$$k_{CR}=M\Sigma_1/(1+H_j)\exp(-(jh\nu_v+\Delta G+\lambda_s)/(4\lambda_s k_B T)) \tag{4}$$

where $M=V^2(4\pi^3/h^2\lambda_s k_s T)^{1/2}$. Here V is identified as the donor–acceptor electronic coupling energy, λ_v is the internal reorganization energy, $H_j=8\pi^2 F_i V^2 \tau_L/(h\lambda_s)$, F_j is a Franck–Condon factor given by $F_j=e^{-s}s^j/j!$ with $s=\lambda_v/h\nu_v$, ν_v is the average frequency of the vibration, and τ_L is the longitudinal relaxation time of the solvent. The best fit of the data is shown in Fig. 7, which yielded $\lambda_s=0.45$ eV and $\tau_L=0.8$ ps. Both sets of data for charge recombination reactions could be generally fit with Eq. (4).

The rate constants of CR for the complex between TMPyP and AZ were shown to be almost independent (1.5 times) of whether the reaction was carried out in neat water or in a 1:1 (v/v) mixture of water and 1-propanol. This small change in the rate indicates that CR is probably not controlled by solvent dynamics, although the use of a mixture of solvents rather than a pure solvent of different relaxation dynamics must remain a cause for concern. Non-exponential decay of the charge-separated state in the TMpyP-AZ complex shows some similarity with data obtained recently for the benzene–Br complex [34]. The charge recombination kinetics in that case were also found to have a weak solvent dependence, a fact that was attributed to significant inner shell reaction in that timescale. In our case, the fact that the data at the top of the plot of log k_{CR} rate constant vs. driving force (Fig. 7) are only weakly affected by solvent dynamics implies another limiting process.

---

[3] No electron transfer couples using components such as those here have been found yet that have ΔG greater than approximately 1.1 eV for the CS reaction, i.e. in the inverted region.

There are similarities between the charge recombination dynamics studied here and the electron transfer (ET) reactions in complexes between dye and solvent molecules studied recently by Yoshihara and coworkers [31]. It was shown [31] that an ultrafast ET reaction takes place from the non-equilibrium state in competition between the ultrafast reaction and the solvation process. The data were rationalized in the terms of an extended Sumi–Marcus [31,38] model, which considers electron transfer reactions in two dimensions. One dimension is the solvation coordinate; the second is a nuclear vibrational coordinate. For this non-equilibrium electron transfer, the non-exponential kinetic profile is highly characteristic [31]. We can assume that the CR reaction studied here also can be considered as a reaction where reactants are in a non-equilibrium state. If this is correct, a model similar to the non-equilibrium electron transfer reaction can be used. Therefore, there is a strong possibility that this putative limiting factor is the vibrational dynamics of the complex.

The data shown in Fig. 7 can be compared with the results of experiments reported from the Mataga group [8] and from Wasielewski and coworkers [7] for porphyrin-based self-associated complexes. The data of Mataga and coworkers show a linear dependence of rate of CR vs. driving force for the electron transfer reaction in porphyrin dimers. This may correspond to one part of the plot in Fig. 7. The data of Wasielewski and coworkers show no ordinal dependence of the CR rate constant on driving force in porphyrin–porphyrin complexes (systems similar to those studied by Mataga and coworkers). In the present work porphyrins were employed as one part of the electron transfer complex only; the second part of the complex was a molecule of smaller physical size. In such a case, the electronic coupling may be stronger [9] than in the cases where both donors and acceptors were both porphyrins.

Acknowledgements

We are grateful to Dr Daniel Houde of the Laboratory of Nuclear Medicine and Radiobiology at the University of Sherbrooke for the use of, and for assistance with, the femtosecond spectrometer. This work is supported in part by the Center for Photochemical Sciences, Bowling Green State University.

References

[1] M. Rougee, T. Ebbesen, F. Ghettl and R.V. Bensasson, *J. Phys. Chem.*, *86* (1982) 4404.I. Okura, S. Aono, M. Hoshino and A. Yamada, *Inorg. Chim. Acta*, *86* (1984) 155.C. Nahor and T. Rabani, *J. Phys. Chem.*, *89* (1985) 2469.J.A. Goodwin and W.R. Scheidt, *J. Phys. Chem.*, *94* (1990) 4432.K. Kemnitz and T. Sakaguchi, *Chem. Phys. Lett.*, *196* (1992) 497.

[2] P.-A. Brugger, M. Gratzel, T. Guarr and G. McLendon, *J. Phys. Chem.*, *86* (1982) 944.

[3] A. Harriman, G. Porter and A. Wilowska, *J. Chem. Soc., Faraday Trans. 2*, *90* (1984) 191.

[4] J.A. Shelnutt, *J. Phys. Chem.*, *88* (1984) 6121.J.A. Shelnutt, *J. Phys. Chem.*, *87* (1983) 605.E. Ojadi, R. Selzer and H. Linschitz, *J. Am. Chem. Soc.*, *107* (1985) 7783.H. van Willigen, U. Das, E. Ojadia and H. Linschitz, *J. Am. Chem. Soc.*, *107* (1985) 7784.

[5] T.H. Tran-Thi, J.F. Lipskier, M. Simoes and S. Palacin, *Thin Solid Films*, *210–211* (1992) 150.

[6] T.H. Tran-Thi, J.F. Lipskier, D. Houde, C. Pepin, E. Keszei and J.P. Jay-Gerin, *J. Chem. Soc., Faraday Trans.*, *88* (1992) 2129.

[7] F.J. Vergeldt, R.M. Koehorst, T.J. Schaafsma, J.-C. Lambry, J.-L. Martin, D.C. Johnson and M.R. Wasielewski, *Chem. Phys. Lett.*, *107* (1991) 182.

[8] H. Segawa, C. Takehora, K. Hinka, T. Shimidzu, T. Asahi and N. Mataga, *J. Phys. Chem.*, *96* (1992) 503.

[9] A.M. Brun, A. Harriman and S. Hubig, *J. Phys. Chem.*, *96* (1992) 254.

[10] S.L. Logunov and M.A.J. Rodgers, *J. Phys. Chem.*, *96* (1992) 8697.

[11] J.S. Zhou and M.A.J. Rodgers, *J. Am. Chem. Soc.*, *113* (1991) 7728.

[12] W.E. Ford and M.A.J. Rodgers, *J. Phys. Chem.*, *95* (1991) 5827.

[13] D. Miller and G. McLendon, *Inorg. Chem.*, *20* (1981) 950.

[14] S.L. Logunov and M.A.J. Rodgers, *J. Phys. Chem.*, *96* (1992) 2915.

[15] T.H. Tran-Thi, J.F. Lipskier, D. Houde, C. Pepin, R. Langlois and S. Palacin, *J. Chem. Soc., Faraday Trans.*, *88* (1992) 2523.

[16] E.P. Ippen and C.V. Shank, in S.L. Shapiro (ed.), *Ultrashort Light Pulses: Picosecond Techniques and Applications*, Springer, New York, 1977, p. 83.

[17] R. Tian and M.A.J. Rodgers, in R.J. Cherry (ed.), *New Techniques of Optical Microscopy and Microspectroscopy*, Macmillan, London, 1991, Chapter 7.

[18] K.M. Kadish, B.G. Maiya and C. Araullo-McAdams, *J. Phys. Chem.*, *95* (1991) 427.K. Kalyansundaram, *Inorg. Chem.*, *23* (1984) 2453.R.L. Brookfield, H. Ellul and H. Harriman, *J. Photochem.*, *31* (1985) 97.U. Hofstra, R.B.M. Koehorst and T.J. Schaafsma, *Magn. Reson. Chem.*, *25* (1987) 1069.R.B.M. Koehorst, U. Hofstra and T.J. Schaafsma, Magn. Reson. Chem., 26 (1988) 167.

[19] F.J. Vergeldt, R.B.M. Koehorst, A. van Hoek and T.J. Schaafsma, *J. Phys. Chem.*, *99* (1995) 4397.

[20] K. Kano, T. Nakajima, M. Takai and S. Hashimoto, *Bull. Chem. Soc. Jpn.*, *60* (1987) 1281.

[21] A. Harriman, M.C. Richoux and P. Neta, *J. Phys. Chem.*, *87* (1983) 4957.A. Harriman, P. Neta and M.C. Richoux, *J. Phys. Chem.*, *90* (1986) 3444.

[22] M.C. Richoux and A. Harriman, *J. Chem. Soc., Faraday Trans. 1*, *78* (1982) 1873.K. Kalyanasundaram and M. Gratzel, *Helv. Chim. Acta*, *63* (1980) 478.

[23] T. Ohno, A. Yoshimura, H. Shioyama and N. Mataga, *J. Phys. Chem.*, *91* (1987) 4365.

[24] B.P. Neri and G.S. Wilson, *Anal. Chem.*, *91* (1969) 607.

[25] R.A. Marcus and N. Sutin, *Biochim. Biophys. Acta*, *811* (1985) 265.G.L.Gaines, M.P. O'Neil, W.A. Svec, M.P. Neimczuk and M.R. Wasielewski, *J. Am. Chem. Soc.*, *113* (1991) 719.

[26] R. Gill and H.I. Stonehill, *J. Chem. Soc.*, (1952) 1845.

[27] T. Kakitani and H. Kakitani, *Biochim. Biophys. Acta*, *635* (1981) 498.A. Warshel, *Proc. Natl. Acad. Sci. USA*, *77* (1980) 3105.C. Kirmaier, D. Holten and W.W. Parson, *Biochim. Biophys. Acta*, *810* (1985) 33.

[28] J. Rodriguez, C. Kirmaier and D. Holten, *J. Am. Chem. Soc.*, *111* (1989) 6500.

[29] J.-H. Fuhrhop and D. Mauzerall, *J. Am. Chem. Soc.*, *91* (1969) 4174.K. Kalyanasundaram and M. Neumann-Spallart, *J. Phys. Chem.*, *86* (1982) 5163.

[30] I.R. Gould, D. Ege, S.L. Mattes and S. Farid, *J. Am. Chem. Soc.*, *109* (1987) 3794.T. Kakitani and N. Mataga, *J. Phys. Chem.*, *89* (1985) 4752.I.R. Gould, D. Ege, J.E. Moser and S. Farid, *J. Am. Chem. Soc.*, *112* (1990) 4290.S.M. Hubig, *J. Phys. Chem.*, *96* (1992) 2903.

[31] Y. Nagasawa, A.P. Yartsev, K. Tominaga, P.B. Bisht, A.E. Johnson and K. Yoshihara, *J. Phys. Chem.*, *99* (1995) 653.

[32] L.A. Summers, *The Bipyridinium Herbicides*, Academic Press, London, 1980, Chapter 4.

[33] S. Hunig, H. Balli, H. Conrad and A. Schott, *Justus Liebigs Ann. Chem.*, *676* (1964) 36.M.E. Zippleis, W.A. Lee and T.C. Bruce, *J. Am. Chem. Soc.*, *108* (1986) 4433.P. Maruthamuthu, L. Venkatsubramanian and P. Dharmalingam, *Bull. Chem. Soc. Jpn.*, *60* (1987) 1113.

[34] A. Hormann, W. Jarzeba and P. Barbara, *J. Phys. Chem.*, *99* (1995) 2006.W. Jarzeba, K. Thakur, A Hormann and P. Barbara, *J. Phys. Chem.*, *99* (1995) 2016.

[35] I. Rips and J. Jortner, *J. Chem. Phys.*, *87* (1987) 2090.

[36] I.R. Gould, R.H. Young, R.E. Moody and S. Farid, *J. Phys. Chem.*, *95* (1991) 2068.

[37] J. Jortner and M.J. Bixon, *J. Chem. Phys.*, *88* (1988) 167.

[38] H. Sumi and R.A. Marcus, *J. Phys. Chem.*, *84* (1986) 4894.